# CERN Summer Students Programme

Project Report

# Simulating Signals in Silicon Sensors

Allan da Silva Jales
Supervisors: Heinrich Schindler, Federico De Benedetti

September 2025

# Contents

# 1 Introduction

Within CERN's Experimental Physics (EP) department, Work Package 1.1 of the R&D programme (EP R&D WP 1.1) is dedicated to the development and characterization of hybrid silicon detectors. A novel technology studied by the group is the Silicon Electron Multiplier (SiEM), an innovative pixel-sensor concept for future detectors that aims to combine fine pitch, internal gain, and radiation hardness[1].

Within this context, this Summer Student project focused on simulation studies of silicon devices using two complementary frameworks — *Synopsys* Sentaurus TCAD and GARFIELD++ — with two main goals:

- Benchmark *Synopsys* Sentaurus TCAD transient *vs.* GARFIELD++: simulate a planar pixel diode with both tools, loading TCAD electrostatic and weighting fields into GARFIELD++ and comparing its Monte Carlo response with the "classical" transient one.

- Simulate and optimize the SiEM device: quantify performance in terms of collected charge and time resolution.

This report documents the methodology for benchmarking a planar pixel diode and the SiEM simulation studies, which provide insights into its optimization.

# 2 *Synopsys* Sentaurus TCAD

*Synopsys* Sentaurus Technology Computer-Aided Design (TCAD) is a suite for semiconductor device simulations [3]. On a user-defined 3D mesh it solves Poisson's equation together with the electron and hole continuity equations using the finite-element method, yielding electrostatic potential maps, carrier densities, currents, and related quantities. The workflow adopted in this work is summarized in Figure 1: from geometry/doping definition and meshing to transient simulations.

The three main outputs we use here are:

- **Electrostatic field**: field map at the operating bias, exported into GARFIELD++ to drive charge transport;

- **Weighting field**: a second electrostatic field is computed by increasing $+\Delta$V the readout electrode. The weighting field is calculated by the difference between both fields, divided by $\Delta V$
- **TCAD transient signal**: current/charge transients from charge deposition, used as a reference for benchmarking against GARFIELD++.

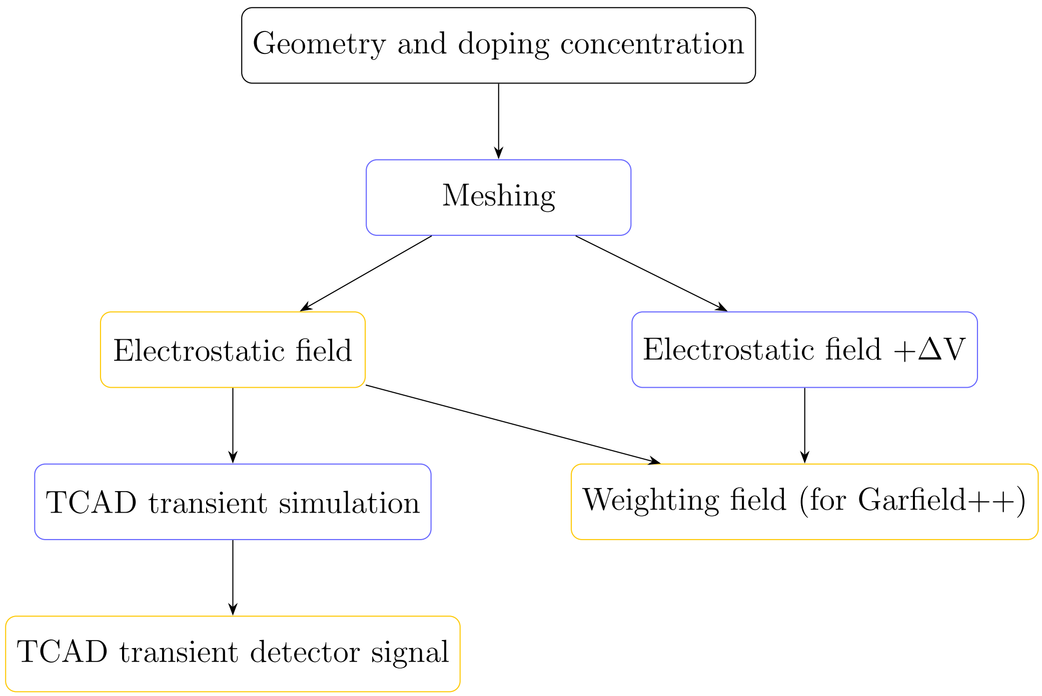


Figure 1: *Synopsys* Sentaurus TCAD workflow. The device geometry and doping profiles are defined, a volume mesh is generated, and two quasi-stationary solutions are computed: (i) the electrostatic field at the chosen bias and (ii) a solution with the readout electrode set to $+\Delta$V to derive the weighting field. A transient simulation with a localized charge deposition yields the TCAD detector signal. The electrostatic and weighting fields are exported and later used as inputs in GARFIELD++.

## 3 Garfield++

GARFIELD++ is an object-oriented toolkit for simulating signal formation in gas-based and semiconductor detectors [2]. In this work it uses user-supplied *electrostatic* and *weighting* fields exported from *Synopsys* Sentaurus TCAD to transport charge carriers with a Monte-Carlo drift model and to compute the induced current. The overall workflow is shown in Figure 2.

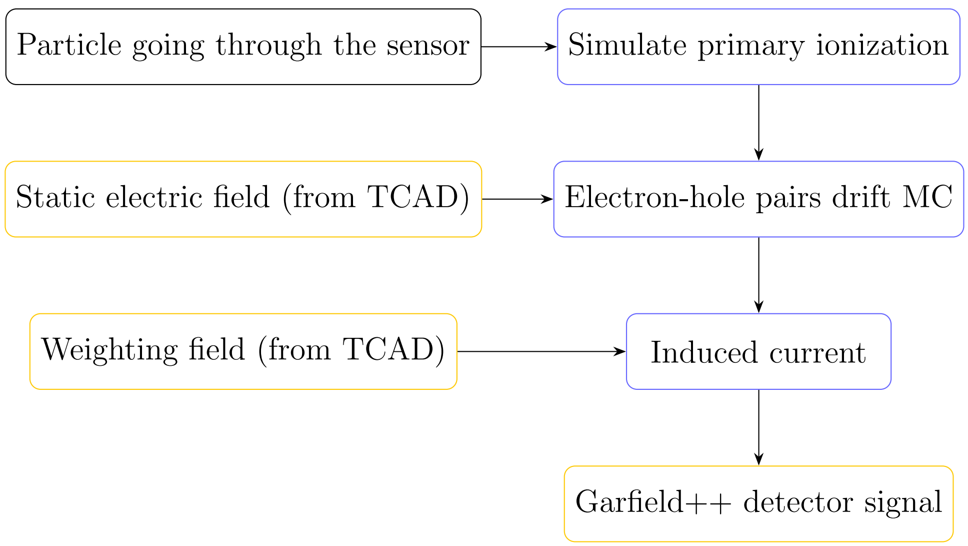


Figure 2: GARFIELD++ workflow used in this report. A primary ionization is generated in the sensor; the electrostatic field from *Synopsys* Sentaurus TCAD drives the Monte-Carlo drift/diffusion of electron–hole pairs; the weighting field from *Synopsys* Sentaurus TCAD is used to compute the induced current, which yields the detector signal.

In this study, all ionization process on GARFIELD++ were caused by a simulated beam of pions at 180 GeV crossing vertically the device. For all checks in the benchmarking process the beam was located on the center of the device.

## 4 Planar Pixel Detector

To benchmark the two simulation chains, we use a well-known device: a planar pixel detector. It is a p–n diode segmented into pixels, with a readout contact on the top (where the signal is measured) and a bulk contact on the bottom (where the reverse bias is applied).

A diode has two regions: an n-type region, with an excess of electrons, and a p-type region, with a deficit of electrons (holes). Where they are in contact, the p–n junction forms and a depletion region appears. Under reverse bias this region widens; ionization due to charge particles in the silicon bulk then creates electron–hole pairs that drift under the electric field and induce a current on the readout contact.

The planar pixel detector used here is presented in Figure 3 and is composed by:

- **Readout contact** (top): electrode where the induced current is measured;
- **Bulk contact** (bottom): electrode used to apply the bias voltage;
- **Silicon bulk**: volume where electron–hole pairs are created;
- **p–n junction line**: interface between the p- and n-type regions;
- **Depletion region**: silicon region where electron-holes pairs are produced and drifted towards readout contact due to electrostatic field.

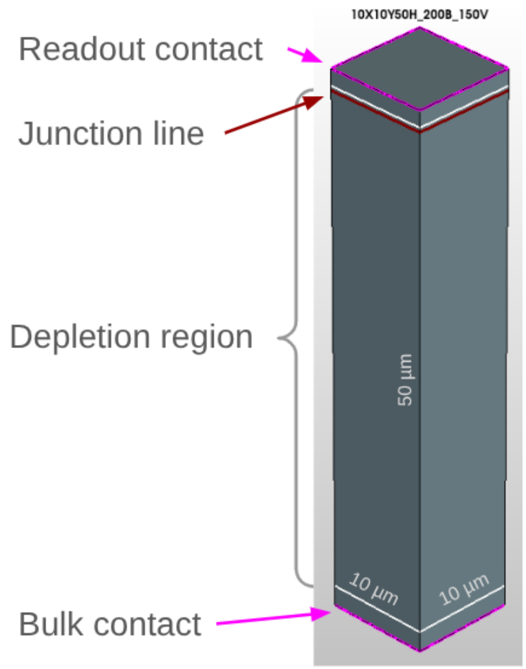


Figure 3: Planar pixel device with pitch $10 \times 10\,\mu\text{m}^2$ and thickness $50\,\mu\text{m}$. The magenta line on top indicates the readout contact; the magenta line at the bottom indicates the bulk contact. The red line marks the junction line, and the white contours delimit the depletion region. The applied reverse bias at the bulk contact is $-200\,\text{V}$.

# 5 Benchmark

With both simulation chains configured, we compared their transient signals results for the planar pixel diode. Figure 4 shows a good agreement of the induced current versus time, with the signal decreasing to zero once all carriers have been collected at the readout electrode. The *Synopsys* Sentaurus TCAD transient required about 1.47 h for one injected track on a dedicated high-end machine, whereas the GARFIELD++ result (an average over 100 events) took less than 1 h on LXPLUS environment.

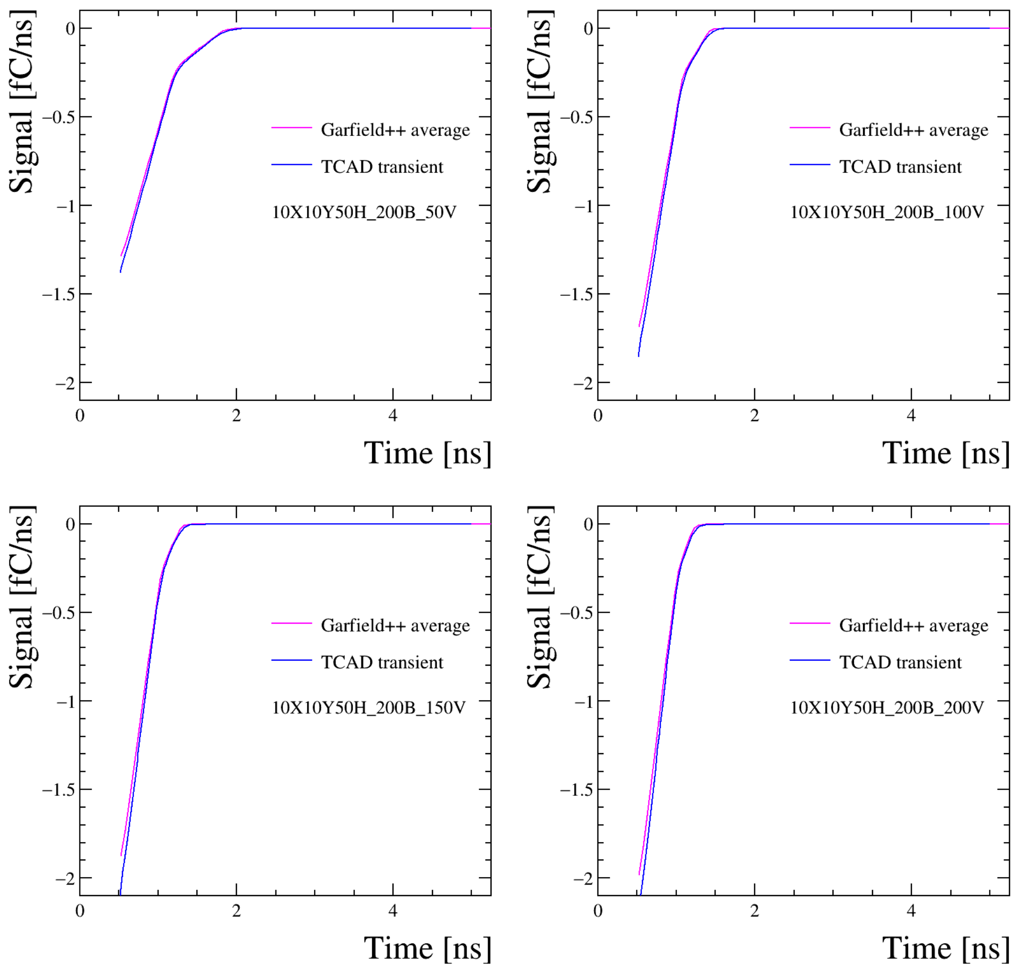


Figure 4: Comparison of GARFIELD++ (magenta, 100-event average) and *Synopsys* Sentaurus TCAD transient (blue) signals for a planar pixel diode at four reverse biases: $-50$ V, $-100$ V, $-150$ V, and $-200$ V.

# 6 Silicon Electron Multiplier

The Silicon Electron Multiplier (SiEM) is a pixel sensor concept designed to combine internal gain, fine pitch and excellent radiation hardness for future tracking detector applications[1]. Its operating principle is illustrated in Figure 5: (1) ionizing particles create electron–hole pairs in the drift region of the silicon bulk; (2) two metal electrodes placed at the bottom of a vertical silicon pillar are biased with a potential difference dV, producing a strong electric field at the pillar base; electrons drifting into this region are multiplied by impact ionization (with gain $\gtrsim 10$) before being collected by the readout electrode through the pillar.

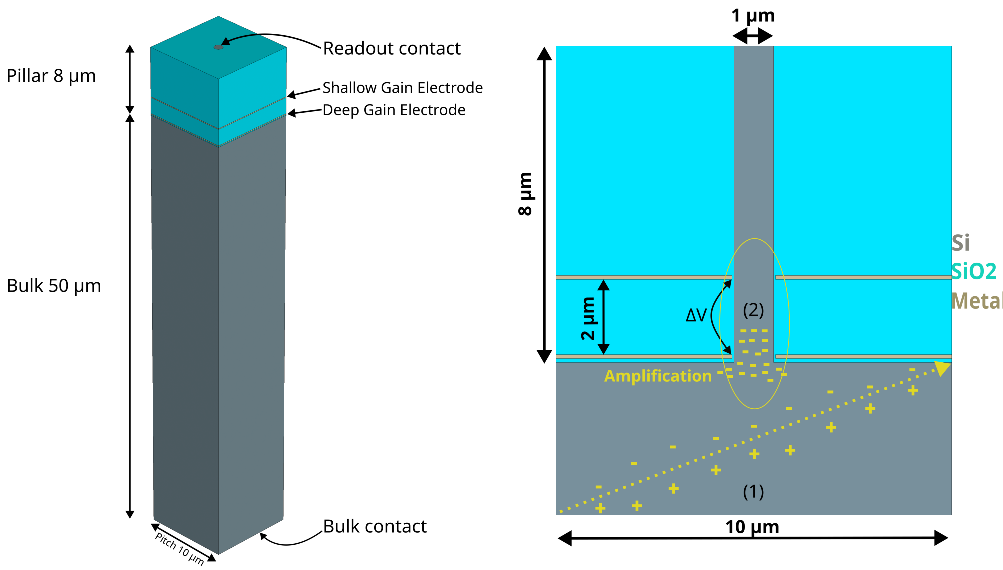


Figure 5: SiEM concept. Left: isometric view highlighting the pillar, the bulk and the two gain electrodes. Right: cross section of the pillar region showing the high-field zone at the base created by a bias dV between the gain electrodes; electrons produced in the drift region (1) are multiplied in (2) and collected at the readout. Materials indicated: Silicon, $SiO_2$, Metal.

From a device perspective, the pillar region is also engineered with a silicon material. The medium around the pillar is made of $SiO_2$ material. The metal electrodes are not in touch with the pillar while the readout electrode sits above the pillar.

The SiEM devices explored in this work are $10 \times 10\ \mu m^2$ pitch and $50\ \mu m$ height for the bulk. The pillar consists of a cylinder or an inverted truncate cone with $8\ \mu m$ height and the base always having $1\ \mu m$ diameter while the diameter of its top (here defined by the letter T) varying. There are two electrodes in this configuration and the specific distance between the electrodes and the pillar is called here *retraction*. It varies and also has a proper symbol: the letter R.

In this project we study the SiEM with a combined *Synopsys* Sentaurus TCAD → GARFIELD++ workflow: *Synopsys* Sentaurus TCAD simulations provide the electrostatic and weighting fields. The fields are then imported into GARFIELD++ to model charge transport and get the induced current with a Monte-Carlo simulation. We scan two geometric parameters: the pillar top diameter (T) and the retraction of the gain electrodes with respect to the pillar wall (R). The performance are then evaluated in terms of collected charge and time resolution on the mean time.

For these studies, we deplete the bulk down to a fixed voltage of $-20\,\mathrm{V}$ and then we ramp the gain electrode dV down until a breakdown condition occurs. The ramp down ensure that the voltage on the bulk is kept constant to $-20\,\mathrm{V}$ during the whole process.

# 7 Time resolution

The mean time is calculated by a weighted average among all the signal of the simulation, the “center of gravity” of the induced current for each simulated track. The Equation 1 describes how each mean time is calculated for each signal.

$$\bar{t} = \frac{\sum_j I_j t_j}{\sum_j t_j} \tag{1}$$

Then, it draws the mean time in a histogram for N simulations. The expected result of the histogram is a gaussian-like distribution. We are using the standard deviation of the “center-of-gravity” time as an estimator of the time resolution.

## 7.1 Gaussian function

The Gaussian function, as known as normal distribution, is one of the most used Probability Density Function (PDF) due its symmetric shape (Figure 6 and the property that most of physical phenomena distribute approximately on this way.

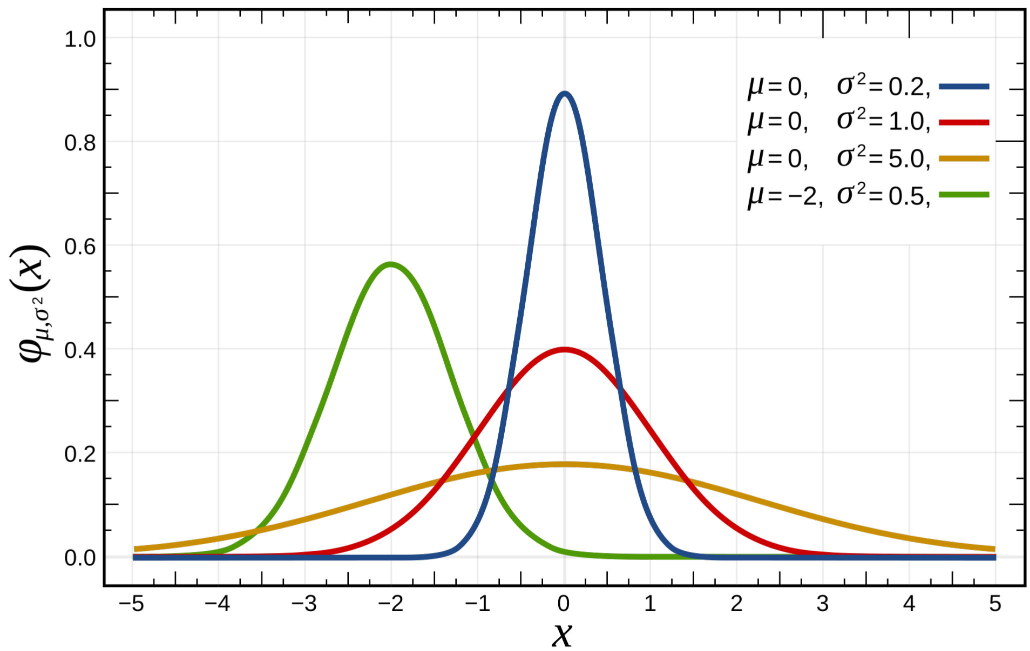


Figure 6: Normalized gaussian function behavior for for different means $\mu$ and variances $\sigma^2$[4].

The general equation of the Gaussian function is described by Equation 2.

$$f(x) = \frac{1}{\sqrt{2\pi\sigma^2}} \exp\left(-\frac{(x-\bar{x})^2}{2\sigma^2}\right) \tag{2}$$

The Gaussian function parameters are:

- $\bar{x}$ (mean): represents the mean value of the distribution. This parameter moves the curve along the $x$ axis. Sometimes are symbolized by the letter $\mu$;
- $\sigma$ (standard deviation): determines the curve width. A large $\sigma$ produces a wider curve and flatter curve, while a smaller $\sigma$ produces a narrower and taller one.

# 8 Comparing different geometries

Each device geometry allow us to deplete down to a certain voltage. Its important to compare the geometries not only at their maximum depletion voltage, but also to compare them with the maximum common gain electrode voltage. The first comparisons are discussed in Section 8.1 and the second one is discussed in Section 8.2.

## 8.1 Maximum possible gain electrode voltage comparison

The Figure 7 shows the results of simulations at maximum possible gain electrode voltage for each geometry. Table 1 shows the main fitting results for the Gaussian function over the mean time histogram.

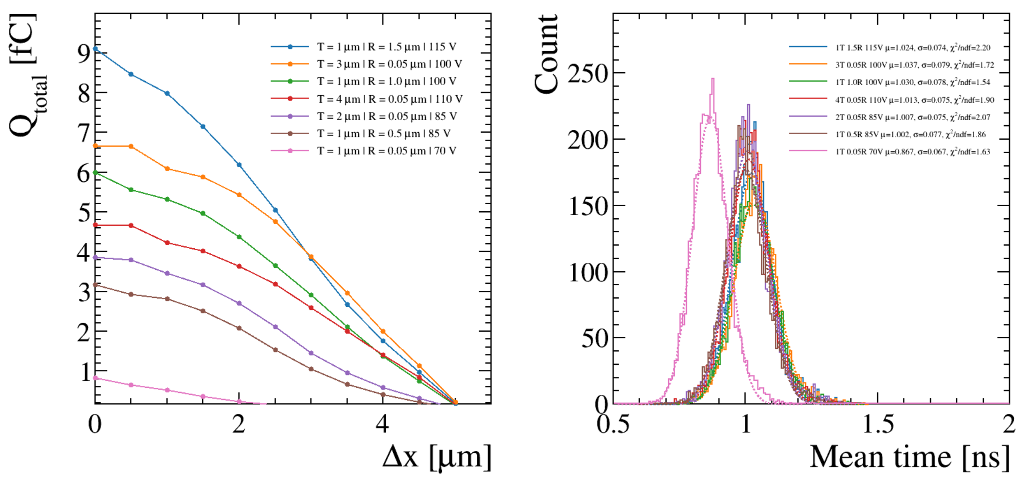


Figure 7: Left: Collected charge vs beam position offset in $x$. Right: Time distribution at $\Delta x = 0$. Both results are estimated with 3000 simulations for each device-position. $x = 0$ means the beam crossed the device vertically in the center of it. When $x = 5\,\mu m$ it means the beam crosses the device at its edge.

| Geometry label | Gain Voltage | $\mu$ | $\sigma$ | $\chi^2$/ndf |
|---|---|---|---|---|
| T = 1 µm \| R = 1.50 µm | 115 V | 1.024 | 0.074 | 2.20 |
| T = 3 µm \| R = 0.05 µm | 100 V | 1.037 | 0.079 | 1.72 |
| T = 1 µm \| R = 1.00 µm | 100 V | 1.030 | 0.078 | 1.54 |
| T = 4 µm \| R = 0.05 µm | 110 V | 1.013 | 0.075 | 1.90 |
| T = 2 µm \| R = 0.05 µm | 85 V | 1.007 | 0.075 | 2.07 |
| T = 1 µm \| R = 0.50 µm | 85 V | 1.002 | 0.077 | 1.86 |
| T = 1 µm \| R = 0.05 µm | 70 V | 0.867 | 0.067 | 1.63 |

Table 1: Table of main fitting results parameters for mean time on maximum possible gain electrode voltage for each device geometry over 3000 simulations for each geometry. The beam crosses the device at $\Delta x = 0$.

As we can see in Table 1, the resolution in time is similar between geometries, except for the T = 1 µm | R = 0.05 µm | 70 V which has a slightly better time resolution and a faster signal.

On the graphs shown in Figure 7, we can see that the T = 1 µm | R = 1.50 µm | 115 V configuration has a higher total charge peak while the T = 3 µm | R = 0.05 µm | 100 V has a less dependence with the $x$ coordinate of injection[1].

## 8.2 Maximum common gain electrode voltage comparison

Figure 8 shows the results of simulations at maximum common gain electrode voltage for each geometry. Table 2 shows the main fitting results for the Gaussian function over the mean time histogram.

[1]In ideal case we would see a flat line, but it is not possible because the electrons generated far from the pillar have to bend into the pillar and some are lost during this drift.

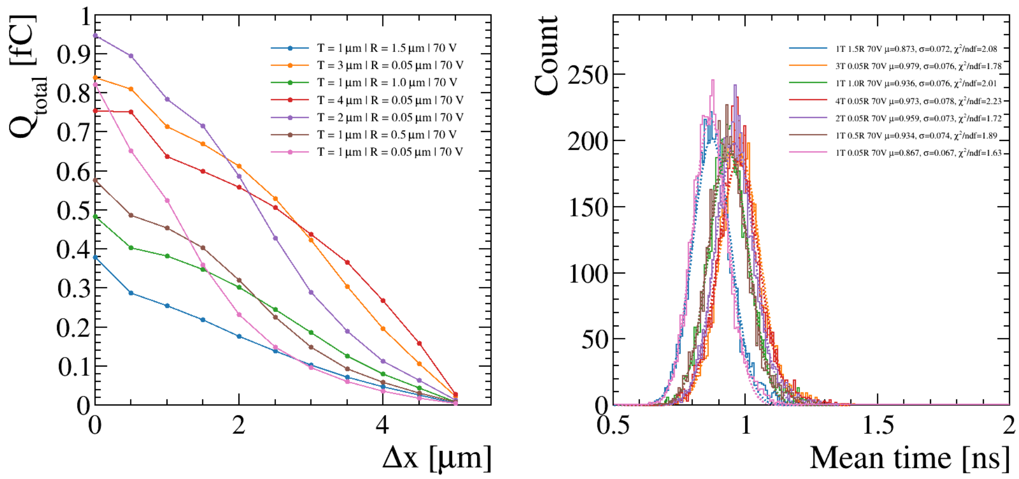


Figure 8: Left: Collected charge vs beam position offset in $x$. Right: Time distribution at $\Delta x = 0$. Both results are estimated with 3000 simulations for each device-position. $x = 0$ means the beam crossed the device vertically in the center of it. When $x = 5\,\mu\text{m}$ it means the beam crosses the device at its edge.

| Geometry label | Gain Voltage | $\mu$ | $\sigma$ | $\chi^2$/ndf |
|---|---|---|---|---|
| T = 1 µm \| R = 1.50 µm | 70 V | 0.873 | 0.072 | 2.08 |
| T = 3 µm \| R = 0.05 µm | 70 V | 0.979 | 0.076 | 1.78 |
| T = 1 µm \| R = 1.00 µm | 70 V | 0.936 | 0.076 | 2.01 |
| T = 4 µm \| R = 0.05 µm | 70 V | 0.973 | 0.078 | 2.23 |
| T = 2 µm \| R = 0.05 µm | 70 V | 0.959 | 0.073 | 1.72 |
| T = 1 µm \| R = 0.50 µm | 70 V | 0.934 | 0.074 | 1.89 |
| T = 1 µm \| R = 0.05 µm | 70 V | 0.867 | 0.067 | 1.63 |

Table 2: Table of main fitting results parameters for mean time on maximum common gain electrode voltage for each device geometry over 3000 simulations for each geometry. The beam crosses the device on $\Delta x = 0$.

Table 2 shows us the same behavior described in the maximum possible gain electrode voltage table: the T = 1 µm | R = 0.05 µm | 70 V has a slightly better resolution time and a faster mean signal. This time, the T = 1 µm | R = 1.50 µm | 70 V geometry has also a faster mean signal, but not as good time resolution as the other one. However, this exactly same geometry on

Figure 8 has the worse total charge collected peak among others and the other one has the worse behavior for total charge collected. The T = 1 µm | R = 0.50 µm | 70 V has highest peak, and the geometries T = 3 µm | R = 0.05 µm | 70 V and T = 4 µm | R = 0.05 µm | 70 V has the best behavior in this case with higher collected charge for $\Delta x \geq 2$.

# 9 Conclusion

This work presents the first systematic Garfield++ study of single-pixel SiEM structures with geometry variations to investigate performance on process variations. Using fields from *Synopsys* Sentaurus TCAD we injected tracks at different lateral offsets $\Delta x$ and analyzed two observables: the total collected charge $Q_{\text{total}}(\Delta x)$ and a time resolution derived from the signal mean time distribution.

For charge collection, Garfield++ enables a direct investigation of how the injection point affects carrier transport and focus it into the pillar. In the "1:1" pillar case (top and bottom widths of 1 µm), a very small gain-electrode retraction (e.g. $R = 0.05$ µm) leads to off-center tracks producing electrons that are less efficiently guided into the pillar, yielding a stronger dependence of Q on $\Delta x$. Increasing the retraction (e.g. R = 0.50 µm) introduces a lateral electric-field component that improves charge focusing, making $Q(\Delta x)$ more uniform. The trade-off is a lower field in the pillar center and thus a reduced gain (smaller total Q). A practical mitigation is to raise the gain-electrode bias: larger retractions tend to shift breakdown to higher voltages, allowing a higher operating point to recover charge while preserving the improved lateral uniformity.

Regarding timing, at $\Delta x = 0$ the geometries studied exhibit similar time resolution within our statistics. A firm conclusion, however, requires mapping both the mean $\mu(\Delta x)$ and the spread $\sigma(\Delta x)$ of the timing metric across the sensor; this can give us precious information to understand what happens with different pillar shapes.

Within the limited scan explored here, the most uniform $Q(\Delta x)$ under both voltage scenarios (Sections 8.1 and 8.2) was observed for the configurations with T = 4 µm | R = 0.05 µm and T = 3 µm | R = 0.05 µm (Figures 7 and 8), while other combinations showed either stronger position dependence or lower peak charge. Overall, Garfield++ proves itself as a valuable way to study how pillar's shape and electrode's retraction together control focusing, gain, and their position dependence.

# References


[1] Marius Mæhlum Halvorsen, Victor Coco, Evangelos Leonidas Gkougkousis, Paula Collins, and Olivier Girard. The silicon electron multiplier sensor. *Nuclear Instruments and Methods in Physics Research Section A: Accelerators, Spectrometers, Detectors and Associated Equipment*, 1041:167325, 2022.

[2] H. Schindler. Garfield++ user guide v2025.1, mar 2025. Online: `https://garfieldpp.web.cern.ch/doxygen/UserGuide.pdf`.

[3] Synopsys. Synopsys tcad. Online: `https://www.synopsys.com/manufacturing/tcad.html`.

[4] Wikimedia. Normal distribution pdf, 2008. Online: `https://commons.wikimedia.org/wiki/File:Normal_Distribution_PDF.svg`.